Batteries & Supercaps

Research Article
doi.org/10.1002/batt.202200280

Chemistry Europe
European Chemical Societies Publishing

www.batteries-supercaps.org

Resolving Graphite-Electrolyte Interphase of Lithium-Ion Batteries using Air-Tight Ambient Mass Spectrometry

Taghi Sahraeian[+],[a] Jingfeng Zheng[+],[a] Remy F. Lalisse[+],[a] Christopher M. Hadad,*[a] Yiying Wu,*[a] and Abraham K. Badu-Tawiah*[a]

The formation of a stable solid electrolyte interphase (SEI) at graphite electrode is necessary for lithium-ion batteries (LIB) to prevent excessive degradation of electrolytes. Until now, the exact organic composition of SEI has not been decisively determined with lithium ethylene mono-carbonate (LEMC) being one of the debated components. An air-tight ambient mass spectrometry (MS) platform is developed to directly characterize the air-sensitive organic components present in SEI. Ionization occurs via a solvent-free field-induced process at atmospheric pressure. Our experimental data, based on tandem MS analysis, revealed LEMC to be the major organic component in SEI. This result resolves a long-standing mystery surrounding the composition of native SEI in LIB, where no trace of the other debated compound, lithium ethylene dicarbonate, was detected. The energetics of fragmentation of LEMC and the corresponding stabilities of various ionic species detected during the air-tight ambient MS analysis were calculated using density functional theory (DFT). Our findings confirmed favorable protonation energies and suggested the molecular structures for many of the detected species. Solvent (i.e., ethylene carbonate)-induced stabilization effects observed during the ionization process were also confirmed by DFT. The reported study encourages the routine use of ambient mass spectrometry to characterize both anodic and cathodic electrodes of all battery types as well as to study other air-sensitive materials in their native state.

Graphite intercalation represents a cornerstone in the development of lithium-ion batteries. During the first few charge/discharge cycles, electrolytes are electrochemically reduced on the surface of graphite, forming a solid-electrolyte interphase (SEI) (Figure 1A, i). A commonly used electrolyte includes $LiPF_6$ (1 M) in a mixture of ethylene carbonate (EC) and dimethyl carbonate (DMC). The as-formed SEI layer is generally ~10 to 50 nm thick, contains inorganic salts (e.g., Li_2CO_3 and LiF) close to the electrode and degraded carbonate molecules (e.g., semi-carbonates and polymers) close to the electrolyte.[1] An ideal SEI layer prevents further electrolyte degradation by acting as an electronic insulator while facilitating Li^+ transport.

Analysis of the SEI layer is challenging due to the physical (ultra-thin) and chemical complexities. Additional complications come from its sensitivity to moisture and oxygen, including changing of its chemical composition within minutes upon exposure to water and/or air. An ideal technique for SEI characterization should satisfy six prerequisites listed in the spider plot in Figure 1(B). One such prerequisite is that sample preparation and analysis should not change the characteristic of the SEI layer. For instance, solvent used in nuclear magnetic resonance (NMR) experiments may trigger chemical conversion of SEI components. In this case, a technique capable of direct analysis with minimum sample preparation would be most useful. Also, the technique needs to be fast and sensitive, while providing molecular-level and morphological information. For instance, surface sensitive X-ray photoelectron spectroscopy (XPS) can only provide information regarding the bonding environment of elements present in a sample. Therefore, although a large variety of analytical techniques, ranging from surface to bulk analysis techniques, such as XPS,[2] Raman,[3] Fourier transform infrared (FT-IR),[4] X-ray powder diffraction (XRD),[5] mass spectrometry (MS),[6] and NMR[1d] have been used to characterize SEI, the true composition and structure of the SEI remain elusive.

MS is a sensitive analytical technique, which directly provides molecular weight and structural information.[7] MS has been applied to study the electrolyte evolution in electrode-electrolyte interphase and in electrolytes.[6] Ambient ionization techniques such as desorption electrospray ionization (DESI)[6c,8] and low-temperature plasma (LTP)[9] allow direct surface analysis under ambient conditions without prior sample treatment. In 2016, Liu and co-workers applied DESI-MS to characterize SEI and cathode-electrolyte interphase (CEI).[6c] In their study, cycled working electrodes were tested without any treatment, which exclude any possible changes during the analysis process. However, their work suffers from two important shortcomings: first, acetonitrile, used as the DESI

[a] T. Sahraeian,[+] J. Zheng,[+] R. F. Lalisse,[+] Prof. C. M. Hadad, Prof. Y. Wu, Prof. A. K. Badu-Tawiah
Department of Chemistry and Biochemistry
The Ohio State University
Columbus, OH-43210 (USA)
E-mail: badu-tawiah.1@osu.edu
wu@chemistry.ohio-state.edu
hadad.1@osu.edu

[+] These authors contribute equally.

Supporting information for this article is available on the WWW under https://doi.org/10.1002/batt.202200280

Research Article
doi.org/10.1002/batt.202200280
Chemistry Europe
European Chemical Societies Publishing

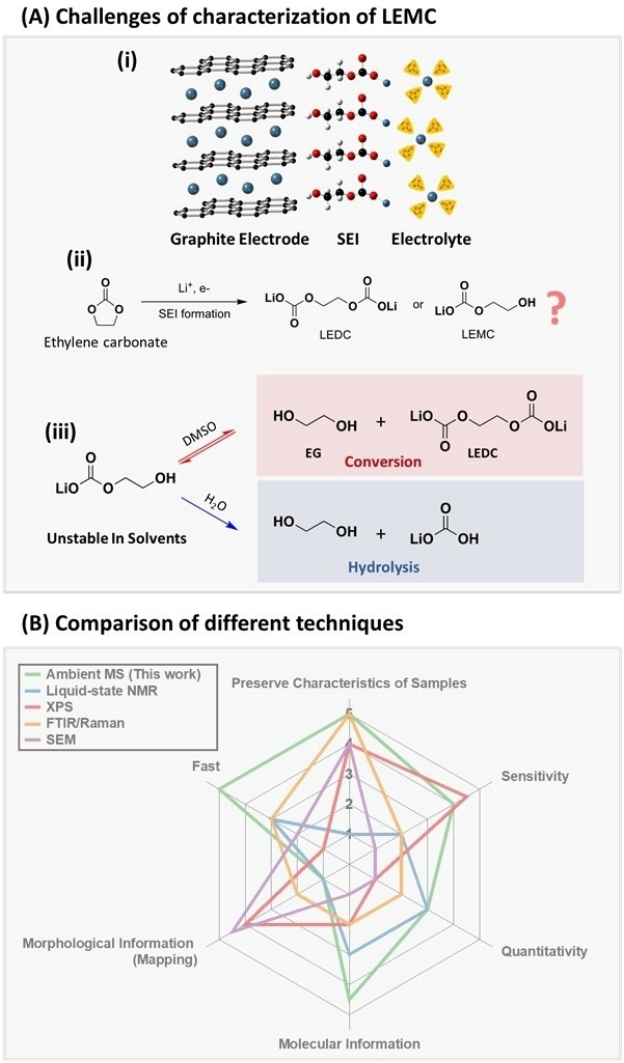

Figure 1. A) The challenges of characterization of organic components such as lithium ethylene mono-carbonate (LEMC) in solid-electrolyte interphase (SEI); (i) schematic showing the SEI layer formed between graphite electrode and electrolyte after battery cycling, (ii) two debated species, lithium ethylene dicarbonate (LEDC) and LEMC, as to which one is the main component of the SEI, (iii) instability of LEMC and LEDC in solvents and their complex equilibria. B) The prerequisites for an ideal characterization technique for SEI layer, comparing merits for different techniques.

spray solvent, may cause changes in SEI composition; and second, the SEI sample was left in open air during DESI-MS analysis, which may cause unwanted sample oxidation or hydrolysis.

In the current study, we developed an ambient ionization platform that can be performed both in ambient air and under air-tight conditions. We have applied this platform to analyze the SEI layer with no sample preparation and more importantly no additional solvent is needed. This allows us to investigate debated SEI compositions and to discover new insights. One notable example is the organic degradation product from EC. In general, it is commonly believed that lithium ethylene dicarbonate (LEDC; Figure 1A, ii), generated from the reduction of EC, is the main organic component in SEI. However, a recent study by Wang and co-workers suggested that the previously reported synthesized LEDC standard is indeed lithium ethylene mono-carbonate (LEMC).[1d] LEMC, instead of LEDC, is more likely to be the main SEI component. In Wang's study, NMR spectroscopic studies, using either DMSO or D_2O as solvents, compared the SEI layer to standards of LEMC and LEDC. However, LEMC and LEDC are involved in complex equilibria that allow rapid interconversions in DMSO and hydrolysis in D_2O (Figure 1A, iii). This instability and conversion in solvents make the analysis and subsequent interpretation of data derived from real SEI samples even more challenging. In 2020, Henschel and co-workers utilized ^{13}C-labeling of electrolyte components to study the electrochemical decomposition of electrolytes.[6d] The authors concluded that LEMC is an integral part of their proposed electrochemical degradation mechanism, although direct experimental evidence was lacking. Similarly, a recent study has used theoretical calculations to predict the presence of LEMC in SEI.[10] Herein, we demonstrate the first direct molecular evidence confirming that LEMC is more likely to be the main organic SEI component for graphite electrodes. Moreover, this new air-tight ambient MS method can also be applied to other battery systems and air-sensitive chemical species.

We first used our new air-tight ambient MS method to characterize standard LEMC that we synthesized following a reported method,[1d] as shown in Scheme S1. The purity of the synthesized material was confirmed using powder X-ray diffraction Figure S1). As mentioned before, ^1H NMR analysis failed to distinguish between the presence of LEMC from LEDC in the DMSO-d_6 solvent, as also described by Wang et al.[1d] Instead, as shown in Figure S2, we confirmed that the synthesized LEMC was converted into EG and LEDC with a dynamic equilibrium in DMSO. Moreover, in D_2O solvent (Figure S3), the synthesized LEMC was totally hydrolyzed into EG and lithium bicarbonate, changing the integrity of LEMC sample. Therefore, addition of solvents should be avoided to reliably characterize LEMC.

The apparatus for performing solvent-free, air-tight direct ionization outside of the vacuum environment of the mass spectrometer is as shown in Figure 2. The inset illustrates the novel ambient ionization process for direct sampling of the organic components in the Li-ion SEI. The cycled graphite electrode on which SEI is formed was cut into a sharp triangular tip and attached to an alligator clip. The application of direct current (DC) high voltage generates a sufficient electric field between the tip of the graphite triangle and the inlet of the mass spectrometer that causes the ejection and ionization of organic compounds present in the SEI. The test was performed using the designed air-tight sample holder to prevent the interference of oxygen and moisture on the samples. We determined, through extensive experiments, that samples (see Supporting Information and Figures S4 and S5 for cycled graphite electrode preparation) kept in the air-tight container can be left for hours without oxidation/decomposition (Figure S6). When ready for MS analysis, the whole container is placed in front of the mass spectrometer, and the front outlet is opened and aligned with the MS inlet, as shown in Figure 2. Just before opening the front outlet, the gas inlet to the air-

Research Article
doi.org/10.1002/batt.202200280

Chemistry Europe
European Chemical Societies Publishing

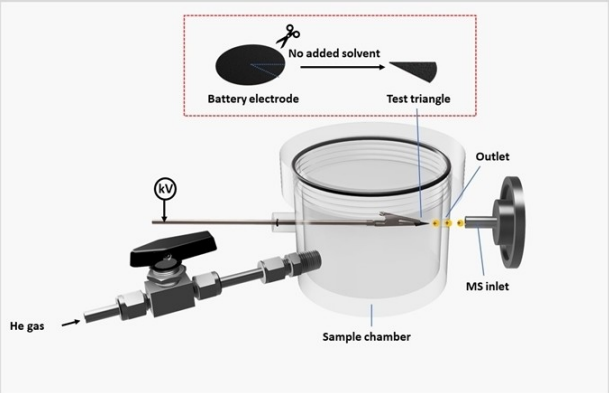

Figure 2. Experimental set-up for direct analysis of battery graphite electrodes with air-tight ambient MS. No solvent is used except of LP30 electrolyte for wetting the surface during preparation in glovebox. The optimized direct current (DC) voltage applied to the sample is 1.8 kV. The He gas (5 psi) with an optimum flow rate of 1 L/min is controlled by a flow meter.

tight container is opened, and He gas (pressure: 5 psi, flow rate: 1 L/min) is employed to generate a positive pressure at the front outlet of the container to prevent air from entering it. The application of an optimized high voltage of 1.8 kV DC (Figure S7) to the graphite triangle generates ions through a mechanism that we believe to involve the combination of field ionization and (micro) plasma ionization. The generated ions are then transferred through ambient air to the proximal mass spectrometer for *in-situ* structural characterization via tandem MS (MS/MS).

Figure 3(A) shows positive-ion mode mass spectrum recorded when the synthesized LEMC was deposited onto the surface of a graphite electrode. Without cycling, the electrolyte ($LiPF_6$ in EC/DMC) should not introduce any chemical change in the composition of SEI layer and thus was used here to wet the graphite electrode before MS analysis. Electrolyte application and the preparation of graphite triangles, including attachment and placement into the air-tight container, were all performed inside an Ar-filled glovebox. Once inside the air-tight container, the samples can be transferred in ambient air without sample degradation. Upon the application of 1.8 kV, we observed gas-phase ions that are directly related to LEMC (MW 112 Da). For example, the highly abundant peak registered at *m/z* 113 is assigned to protonated LEMC species, which readily loses water (MW 18 Da) and CO_2 (MW 44 Da) during the ionization process to give peaks at *m/z* 95 and 69, respectively, in the single-stage full mass spectrum. The product-ion MS/MS spectra for ions at *m/z* 113 and 95 are provided as inserts in Figure 3(A). As can be observed, the protonated LEMC fragments upon activation in collision-induced dissociation (CID) experiments performed under high vacuum environment of the mass spectrometer to yield fragment ions at *m/z* 95 (major) and 65 through the loss of water and formaldehyde ($CH_2=O$; MW 30 Da), respectively (Figure 3A, i). While CID of species at *m/z* 95 generated during the ionization process at atmospheric pressure fragmented by losing neutral formaldehyde to give ion at *m/z* 65, the same activation process was also found to facilitate a hydration reaction yielding a product ion at *m/z* 113 in the gas phase

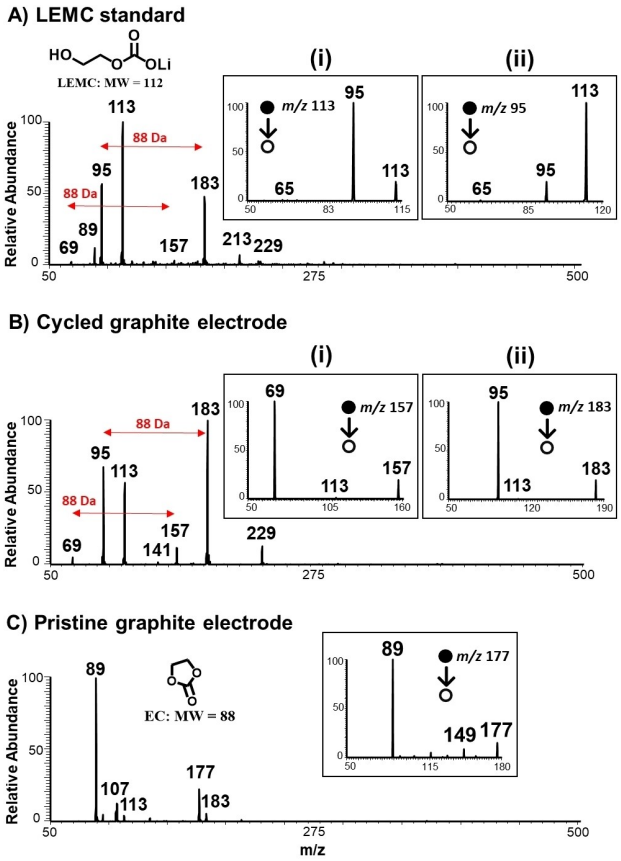

Figure 3. Positive-ion mode mass spectra of different graphite electrode triangle samples. Analysis of A) standard LEMC deposited on pristine graphite, B) cycled graphite electrode with established SEI layer, and C) pristine graphite electrode only with LP30 electrolyte wetting the surface. The insets (i), and (ii) in (A) show typical tandem mass spectra (MS/MS) for species at *m/z* 113 and 95, respectively, for samples containing LEMC. Insert (i) and (ii) in (B) show typical MS/MS for species at *m/z* 157 and 183, respectively, detected in samples containing LEMC. The inset in (C) shows MS/MS at *m/z* 177 indicating the presence of a proton-bound-dimer of the ethylene carbonate (EC) solvent.

(Figure 3A, ii). These two tandem MS experiments confirm that the ions at *m/z* 113 and 95 generated during the air-tight ambient MS experiments are related, both of which originate from the purely synthesized LEMC compound. Additional peaks were observed including peaks at *m/z* 157 and 183, which we ascribe to ethylene carbonate (MW 88 Da) solvent adducts of species at *m/z* 69 and 95, respectively. This assignment is confirmed by tandem MS experiments via CID in which ions at *m/z* 157 fragmented to give a predominant species at *m/z* 69 through the loss of neutral ethylene carbonate (Figure 3B, i). Likewise, MS/MS at *m/z* 183 afforded a major fragment at *m/z* 95 via the loss of neutral ethylene carbonate (Figure 3B, ii). These species were also confirmed via the isotope distributions in the full mass spectra to contain Li, which involve Li-6 and Li-7 at ~1:12 ratios (Figure S8).

After the analysis of the pure LEMC sample, we proceeded to apply the air-tight ambient MS platform to characterize the chemical composition of real SEI samples derived from cycling of Li-ion battery. The graphite electrode is the main component of interest. We used LP30 electrolyte which is a composition of

1 M $LiPF_6$ EC/DMC (vol% 50:50). After battery cycling, the graphite electrode containing the as-formed SEI was removed from the coin cell and cut to a triangular tip, which was subsequently attached to an alligator clip and inside the air-tight container. Here too, all assembly was done inside an Ar-filled glovebox with the aim to maintain SEI integrity before MS analysis. The positive-ion mode mass spectrum derived from the analysis of the cycled graphite electrode is shown in Figure 3(B). Compared with standard LEMC analysis (Figure 3A), all of the expected LEMC-related peaks were observed, including *m/z* 183, 157, 113, 95, and 69. MS/MS experiments confirmed identical structures, as previously deduced for the standard peaks. For purpose of comparison, we provide the mass spectrum (Figure 3C) recorded from the analysis of graphite electrode, wetted with just $LiPF_6$ in EC/DMC electrolyte, but without battery cycling. In this case, the air-tight ambient MS analysis showed peaks at *m/z* 89 and 177, corresponding to protonated EC and proton-bound dimer of EC, respectively. Low abundance peaks at *m/z* 113 and 183 were detected in the pristine graphite electrode; however, their MS/MS spectra (Figure S9) did not match any of the diagnostic fragment ions expected for LEMC related peaks. We further performed two control experiments to investigate the effect of other constitutive parts of the Li-ion battery and SEI samples: analysis of Cu foil alone and dry pristine graphite electrode. The results of these control experiments are shown in Figure S10(A and B), which indicate that neither the Cu itself nor the addition of graphite on Cu produce interpretable peaks related to experiments where SEI was present on the cycled graphite electrode. The obvious chemical difference between spectra before and after cycling (despite common starting materials) confirm the well-known collective changes/reactions that occur to produce SEI during Li-ion battery cycling. Likewise, the high degree of similarities in chemical profiles between spectra derived from the standard LEMC and experimental samples provide strong evidence for the formation of LEMC as the main organic component in Li-ion SEI.

We conducted similar MS analyses of the graphite electrode (with and without cycling) under ambient conditions, without the air-tight container. Under this experimental condition, we could observe the expected native SEI organic constituents immediately or within two minutes of exposure of the sample to ambient air (Figure S11A). However, the expected diagnostic peaks disappeared after longer (>2 min) exposure times (Figure S11B). For comparison purposes, analysis of SEI of cycled graphite sample immediately or after longer residence time (5 min) inside the air-tight container are provided in Figures S11(C and D), which show the same diagnostic peaks as observed for standard LEMC. This result is consistent with the fact that SEI is well known to be unstable in air/moisture, making the design and development of air-tight chamber both necessary and important. The chamber facilitates transport of sample between different laboratories enabling otherwise difficult collaborations to be achieved. With this air-tight MS platform, it is possible to analyze other air/moisture-sensitive samples in their native state. We note that the air-tight ambient ionization source works well at low He carrier gas flow rates (e.g., 1 L/min). Higher gas flow rates were observed to reduce signal-to-noise ratio due to the onset of discharge. Applied DC voltages greater than 1.8 kV also caused excessive discharge, which made it challenging to discern ion peaks due to organic species desorbed from the SEI.

Lastly, we used DFT (B3LYP/6-311+G(d,p); see Supporting Information for details) calculations to evaluate possible MS fragmentation pathways of LEMC by computing the relative free energies of different thermodynamic pathways with Gaussian.[11] We sought to calculate the minimum energy required to cause the loss of water and CO_2 from LEMC, and to investigate other possible fragmentation pathways that might favorably compete with the observed reactions. The optimized geometry of neutral LEMC showed stable structure in which the lithium is bonded between the end OH group and ether oxygen atom (Figure S12). This geometry leaves the carboxylic functional group free to engage in reactions. The proton affinity of the optimized LEMC structure was estimated to be 112.6 kcal/mol (4.88 eV). The fact that protonated LEMC species are detected with ease suggest that (i) field ionization is important in the process and/or (ii) the ionizing particles are highly acidic in nature, including the presence of low molecular weight protonated water clusters $[H^+ (H_2O)_n; n=1, \text{ or } 2]$.[12] Similarly, the optimized structure was used to calculate the ionization potential of LEMC, which was found to be 221.6 kcal/mol (9.61 eV). Note: typically, the breakdown of ambient air to generate corona discharge occurs when DC voltage ≥ 4 kV is applied. Electrons in such electrical discharge are found to have <9 eV of kinetic energy. The 1.8 kV DC voltage used in our experiment ensures that harsh corona discharge is avoided, suggesting that electron energies involved in our experiment are not sufficient to ionize LEMC. However, the numerous collisions occurring at atmospheric pressure can provide the critical energy (<4 eV for most organic compounds) needed to cause fragmentation of LEMC, as observed for the loss of water and CO_2 neutral species.

Our DFT calculations (shown in Figure 4) suggest that the loss of water from the protonated LEMC (*m/z* 113, Figure S13) gives species at *m/z* 95, which is only 11.8 kcal/mol (0.5 eV) less stable than the parent protonated ion (Figure 4A). Also, the fragment ion formed from the elimination of CO_2 from protonated LEMC was found to be 16.4 kcal/mol more stable than the original protonated species at *m/z* 113 (Figure 4B). Possible fragmentation pathways of LEMC, its different reactions with other species, and their energetics are depicted in Figures S14–S20. The release of ethylene oxide (MW 44 Da) from protonated LEMC is another possible pathway through which the species at *m/z* 69 can be formed (Figure 4C). However, this pathway involving ethylene oxide generates ionic species that is 35.6 kcal/mol less stable than the parent protonated LEMC compound. The stability and energetics of the EC adducts at *m/z* 157 and 183 associated with species at *m/z* 69 and 95, respectively, were also investigated (Figure 4). That is, the attachment of EC solvent to ions at *m/z* 69 (at energy -16.4 kcal/mol, after loss of CO_2 from protonated LEMC) produces species (*m/z* 157) of energy -19.8 kcal/mol. This means, the adduct formed between EC and ion at *m/z* 69

Research Article
doi.org/10.1002/batt.202200280
Chemistry Europe
European Chemical Societies Publishing

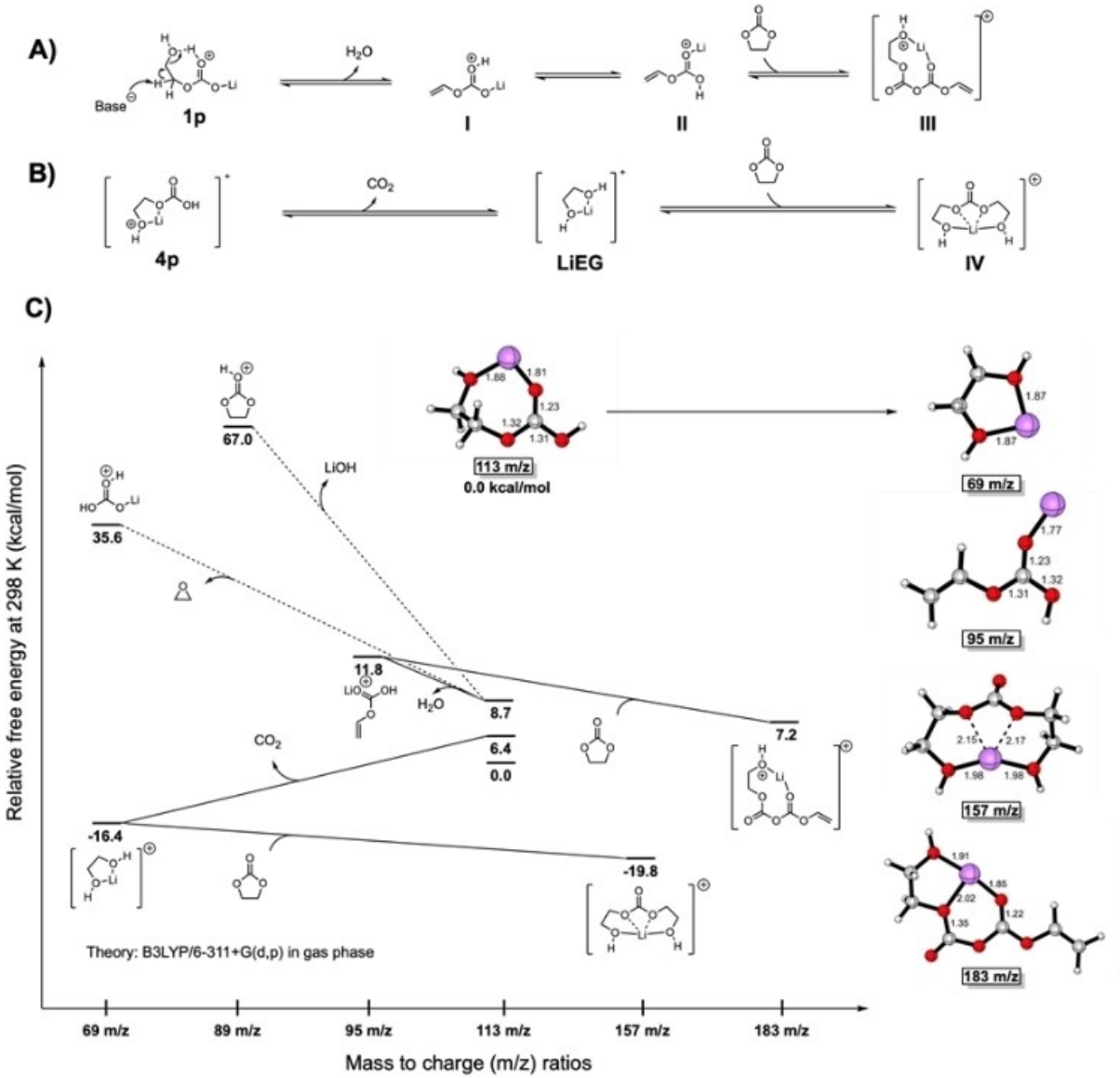

Figure 4. DFT calculations for optimized LEMC (*m/z* 113) structure and several possible pathways leading to species at A) 95 and 183 *m/z* or B) 69 and 157 *m/z*. C) The relative free energies, in kcal/mol at the B3LYP/6-311 + G(d,p) level of theory in the gas phase, are shown in bold text for each pathway that corresponds to the calculated *m/z*.

is approximately 20 kcal/mol more stable than the parent protonated LEMC. Likewise, the attachment of EC solvent to species at *m/z* 95 (at energy +11.8 kcal/mol, after loss of H_2O from protonated LEMC) produces species (*m/z* 183) that is +7.2 kcal/mol less stable than the parent LEMC ion at *m/z* 113. Although results from the DFT calculations correlate well with species detected in our air-tight ambient MS platform, intensities of the species in the recorded mass spectra do not correspond directly to their abundance in the SEI or calculated energetics. This is because ion intensities are influenced by the intrinsic ionization efficiencies of each species, transfer efficiency from the graphite surface to the mass spectrometer, and mass range within which the specific ions are analyzed within the ion trap mass spectrometer.

In summary, the solid electrolyte interphase is an integral part of the Li-ion batteries that can give important insight into the structure and dynamics at graphite electrode. In this study, we have shown that the debated species present in SEI layer at graphite electrode can be detected and characterized by a novel air-tight ambient mass spectrometry technique. In this case, we confirmed that lithium ethylene mono-carbonate is the main organic component as opposed to lithium ethylene dicarbonate. Our method avoids the use of reactive solvents (e.g., water and dimethyl sulfoxide), which typically trigger unwanted hydrolysis or equilibrium reaction that change the identity of the native sample. In addition, our method prevents exposure to ambient air during MS analysis by creating a positive pressure at the outlet of the air-tight container. Collectively, the analytical method presented in this work

enables novel measurements to be made, one that facilitates direct analysis of air-sensitive materials generating molecular information in a non-destructive and rapid manner. DFT analysis, predicting the relative thermodynamic stability of different molecules and ionic species, including fragments and adducts generated from the SEI, provide molecular-level structures that support the detected masses from the air-tight ambient mass spectrometry strategy. Thus, this mass spectrometric approach can afford predictable results. Therefore, we believe that the new MS platform can be applied to analyze other air-sensitive materials to advance important fundamental studies.

Acknowledgements

This research was supported by the Department of Chemistry and Biochemistry, The Ohio State University. AB-T acknowledges the U.S. Department of Energy, Office of Science, Office of Basic Energy Sciences, Condensed Phase and Interfacial Molecular Science (award number DE-SC0022097) for additional support. CMH acknowledges generous computational resources from The Ohio Supercomputer Center.

Conflict of Interest

The authors declare no conflict of interest.

Data Availability Statement

The data that support the findings of this study are available from the corresponding author upon reasonable request.

Keywords: air-tight analysis · ambient ionization mass spectrometry · graphite · lithium-ion batteries · lithium ethylene mono-carbonate · solid-electrolyte interphase

[1] a) R. Yazami, Ph. Touzain, *J. Power Sources* **1983**, *9*, 365–371; b) E. Peled, S. Menkin, *J. Electrochem. Soc.* **2017**, *164*, A1703–A1719; c) E. Peled, *J. Electrochem. Soc.* **1979**, *126*, 2047–2051; d) L. Wang, A. Menakath, F. Han, Y. Wang, P. Y. Zavalij, K. J. Gaskell, O. Borodin, D. Iuga, S. P. Brown, C. Wang, K. Xu, B. W. Eichhorn, *Nat. Chem.* **2019**, *11*, 789–796.

[2] a) A. M. Andersson, A. Henningson, H. Siegbahn, U. Jansson, K. Edström, *J. Power Sources* **2003**, *119–121*, 522–527; b) S. Leroy, F. Blanchard, R. Dedryvère, H. Martinez, B. Carré, D. Lemordant, D. Gonbeau, *Surf. Interface Anal.* **2005**, *37*, 773–781.

[3] a) J.-C. Panitz, F. Joho, P. Novak, *Appl. Spectrosc.* **1999**, *53*, 1188–1199; b) E. Markervich, G. Salitra, M. D. Levi, D. Aurbach, *J. Power Sources* **2005**, *146*, 146–150.

[4] a) S. Geniès, R. Yazami, J. Garden, J. C. Frison, *Synth. Met.* **1998**, *93*, 77–82; b) D. Aurbach, B. Markovsky, I. Weissman, E. Levi, Y. Ein-Eli, *Electrochim. Acta* **1999**, *45*, 67–86.

[5] N. A. Cañas, P. Einsiedel, O. T. Freitag, C. Heim, M. Steinhauer, D.-W. Park, K. A. Friedrich, *Carbon* **2017**, *116*, 255–263.

[6] a) E. Peled, D. Bar Tow, A. Merson, A. Gladkich, L. Burstein, D. Golodnitsky, in *J. Power Sources*, Elsevier, **2001**, pp. 52–57; b) E. Peled, D. Golodnitsky, A. Ulus, V. Yufit, *Electrochim. Acta, Pergamon* **2004**, 391–395; c) Y. M. Liu, B. G. Nicolau, J. L. Esbenshade, A. A. Gewirth, *Anal. Chem.* **2016**, *88*, 7171–7177; d) J. Henschel, C. Peschel, S. Klein, F. Horsthemke, M. Winter, S. Nowak, *Angew. Chem. Int. Ed.* **2020**, *59*, 6128–6137; *Angew. Chem.* **2020**, *132*, 6184–6193; e) S. Laruelle, S. Pilard, P. Guenot, S. Grugeon, J.-M. Tarascon, *J. Electrochem. Soc.* **2004**, *151*, A1202; f) G. Gachot, S. Grugeon, M. Armand, S. Pilard, P. Guenot, J. M. Tarascon, S. Laruelle, *J. Power Sources* **2008**, *178*, 409–421; g) G. Gachot, P. Ribière, D. Mathiron, S. Grugeon, M. Armand, J. B. Leriche, S. Pilard, S. Laruelle, *Anal. Chem.* **2011**, *83*, 478–485; h) H. Wang, E. Rus, T. Sakuraba, J. Kikuchi, Y. Kiya, H. D. Abruna, *Anal. Chem.* **2014**, *86*, 6197–6201; i) E. Castel, E. J. Berg, M. el Kazzi, P. Novák, C. Villevieille, *Chem. Mater.* **2014**, *26*, 5051–5057; j) F. la Mantia, P. Novák, *Electrochem. Solid St.* **2008**, *11*, A84–A87; k) R. Imhof, P. Novák, *J. Electrochem. Soc.* **1999**, *146*, 1702–1706; l) M. Leißing, C. Peschel, F. Horsthemke, S. Wiemers-Meyer, M. Winter, S. Nowak, *Batteries & Supercaps* **2021**, *4*, 1731–1738; m) C. Peschel, F. Horsthemke, M. Leißing, S. Wiemers-Meyer, J. Henschel, M. Winter, S. Nowak, *Batteries & Supercaps* **2020**, *3*, 1183–1192.

[7] a) D. S. Kulyk, Q. Wan, T. Sahraeian, A. K. Badu-Tawiah, *Int. J. Mass Spectrom.* **2022**, *476*, 116836; b) D. S. Kulyk, T. Sahraeian, S. Lee, A. K. Badu-Tawiah, *Anal. Chem.* **2021**, *93*, 13632–13640; c) D. S. Kulyk, T. Sahraeian, Q. Wan, A. K. Badu-Tawiah, *Anal. Chem.* **2019**, *91*, 6790–6799; d) D. S. Kulyk, D. J. Swiner, T. Sahraeian, A. K. Badu-Tawiah, *Anal. Chem.* **2019**, *91*, 11562–11568; e) E. L. Rossini, D. S. Kulyk, E. Ansu-Gyeabourh, T. Sahraeian, H. R. Pezza, A. K. Badu-Tawiah, *J. Am. Soc. Mass Spectrom.* **2020**, *31*, 1212–1222.

[8] a) Z. Takáts, J. M. Wiseman, B. Gologan, R. G. Cooks, *Science* **2004**, *306*, 471–473; b) T. Sahraeian, D. S. Kulyk, A. K. Badu-Tawiah, *Langmuir* **2019**, *35*, 14451–14457.

[9] B. Vortmann, S. Nowak, C. Engelhard, *Anal. Chem.* **2013**, *85*, 3433–3438.

[10] X. Xie, E. W. Clark Spotte-Smith, M. Wen, H. D. Patel, S. M. Blau, K. A. Persson, *J. Am. Chem. Soc.* **2021**, *143*, 13245–13258.

[11] Gaussian 16, (Revision C.01), M. J. Frisch, G. W. Trucks, H. B. Schlegel, G. E. Scuseria, M. A. Robb, J. R. Cheeseman, G. Scalmani, V. Barone, G. A. Petersson, H. Nakatsuji, X. Li, M. Caricato, A. V. Marenich, J. Bloino, B. G. Janesko, R. Gomperts, B. Mennucci, H. P. Hratchian, J. V. Ortiz, A. F. Izmaylov, J. L. Sonnenberg, D. Williams-Young, F. Ding, F. Lipparini, F. Egidi, J. Goings, B. Peng, A. Petrone, T. Henderson, D. Ranasinghe, V. G. Zakrzewski, J. Gao, N. Rega, G. Zheng, W. Liang, M. Hada, M. Ehara, K. Toyota, R. Fukuda, J. Hasegawa, M. Ishida, T. Nakajima, Y. Honda, O. Kitao, H. Nakai, T. Vreven, K. Throssell, J. A. Montgomery, Jr., J. E. Peralta, F. Ogliaro, M. J. Bearpark, J. J. Heyd, E. N. Brothers, K. N. Kudin, V. N. Staroverov, T. A. Keith, R. Kobayashi, J. Normand, K. Raghavachari, A. P. Rendell, J. C. Burant, S. S. Iyengar, J. Tomasi, M. Cossi, J. M. Millam, M. Klene, C. Adamo, R. Cammi, J. W. Ochterski, R. L. Martin, K. Morokuma, O. Farkas, J. B. Foresman, and D. J. Fox, Gaussian, Inc., Wallingford CT, **2016**.

[12] K. Sekimoto, M. Takayama, *Eur. Phys. J. D* **2010**, *60*, 589–599.

Manuscript received: June 21, 2022
Revised manuscript received: August 2, 2022
Accepted manuscript online: August 4, 2022
Version of record online: August 30, 2022